PHYSICAL REVIEW C VOLUME 27, NUMBER 1 JANUARY 1983

Inelastic excitation and spin flip in heavy ion reactions

S. Chakravarti, P. J. Ellis, and B. F. Bayman
School of Physics and Astronomy, University of Minnesota, Minneapolis, Minnesota 55455

Q. K. K. Liu
Hahn-Meitner-Institut für Kernforschung GmbH, Berlin, Federal Republic of Germany
(Received 2 June 1982)

Coupled channel calculations were carried out for the inelastic scattering of ^{13}C on ^{24}Mg using form factors generated in a single folding model. We studied the population probability P_1 for ^{24}Mg in the 1.37 MeV 2^+ level with $|m|=1$ and ^{13}C in its ground state. Using spin-independent potentials the excitation of various states in ^{13}C gave rise to a maximum $P_1(6°)$ of 0.2%. This increased to 0.3% when spin-dependence was allowed for in an approximate manner. At 10° the calculations fell significantly short of the experimental data. Large polarizations were found when excited states of ^{13}C were populated; these effects are discussed.

[NUCLEAR REACTIONS $^{13}C+^{24}Mg$ inelastic scattering, $E=35$ MeV; coupled channel study of $|m|=1$ population probability for the ^{24}Mg 1.37 MeV 2^+ level and polarization phenomena.]

I. INTRODUCTION

In general the interaction between two nuclei depends upon their separation and on their orientation relative to each other and to the line connecting their mass centers. This orientation dependence is colloquially called "spin dependence," although its physical origin is probably more closely associated with nonsphericity of the nuclear mass density than with interactions involving the intrinsic spin. Indirect evidence for orientation-dependent interactions is provided by the study[1,2] of nucleon transfer between heavy ions. In order to understand the observed angular distributions, it is necessary to assume that the optical potentials governing the relative motion of the nuclei contain a "spin-orbit" term, $\vec{l}\cdot(\vec{I}+\vec{s})$ ($\vec{l}$ is the relative orbital angular momentum and $\vec{I}$ and $\vec{s}$ are the nuclear angular momenta). More direct evidence for orientation-dependent interactions was revealed[3,4] in the study of the reaction $^{24}Mg(0^+)+^{13}C(\frac{1}{2}^-)\rightarrow{}^{24}Mg(2^+)+^{13}C(\frac{1}{2}^-)$. Events were identified in which the component of the ^{13}C angular momentum perpendicular to the reaction plane was reversed as a result of the collision. Similar "spin-flip" measurements[5] have been performed for ^{13}C and ^{15}N incident on ^{12}C. Polarized beams of the "light heavy ions" ^6Li and ^7Li are now available, and vector analyzing powers have been measured for various targets.

Attempts have been made[7] to calculate the orientation-dependent part of the interaction by double folding the nucleon-nucleon spin-orbit interaction over the spin distributions of the two nuclei. These double-folding potentials underpredict the ^{13}C, ^{15}N spin-flip data by several orders of magnitude. They sometimes account for the observed vector-analyzing power,[8] but their predictions are too small for ^6Li incident on ^{58}Ni and ^4He targets,[8,9] and the predicted sign of the vector analyzing power is incorrect for ^7Li on a ^{58}Ni target.[10]

The use of the double-folding model implies that the colliding nuclei remain in their ground states throughout the collision. We know that this does not happen. Excited states of both the projectile and target are populated as the nuclei approach each other, even in cases where one or both nuclei emerge in their ground states. This can allow the angular momentum of the projectile to be flipped, even in the absence of explicitly spin-dependent interactions, i.e., this generates an effective potential which is orientation dependent.

In this paper, we study such effects for the $^{13}C+^{24}Mg$ system. The low-lying states of ^{24}Mg can be described as rotational excitations of a deformed intrinsic shape. The optical potential produced by this deformed mass distribution is nonspherical. We treat the low-lying states of ^{13}C in terms of the spherical shell model. When ^{13}C and ^{24}Mg collide, each ^{13}C nucleon feels the nonspherical ^{24}Mg optical potential. This results in the ^{13}C and ^{24}Mg exerting torques on each other, which leads to the population of the rotational excitations in ^{24}Mg,

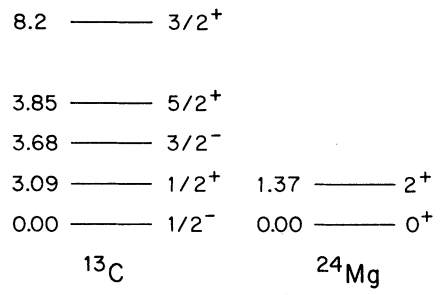

FIG. 1. States of ^{13}C and ^{24}Mg which are included in this calculation. Excitation energies are in MeV. Diagram is not drawn to scale.

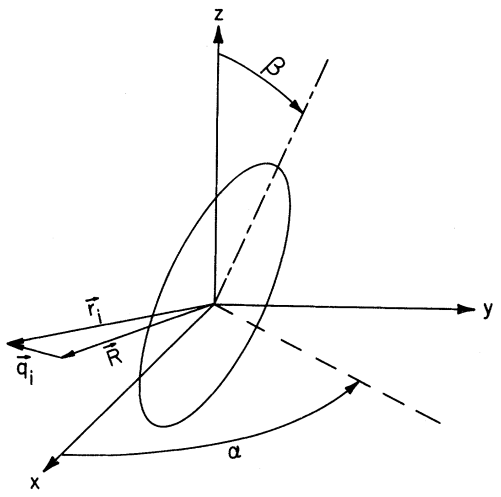

FIG. 2. The angles (β,α) are the polar coordinates of the symmetry axis of the deformed ^{24}Mg nucleus. The mass center of ^{13}C is located relative to the mass center of ^{24}Mg by the vector $\vec{R}$, and $\vec{q}_i$ and $\vec{r}_i$ locate the ith nucleon of ^{13}C with respect to the mass centers of ^{13}C and ^{24}Mg, respectively.

and excited shell-model states in ^{13}C illustrated in Fig. 1. Of course, ^{13}C can emerge in its $\frac{1}{2}^-$ ground state, but even if it does, there is a possibility that its angular momentum component perpendicular to the reaction plane will have been flipped relative to its initial orientation. In this way we can calculate a spin-flip probability to compare with the data of Refs. 3 and 4.

Our calculation proceeds in two stages. We first calculate the ^{24}Mg-^{13}C nucleus-nucleus interaction by folding the deformed ^{24}Mg optical potential over the 13 nucleon shell-model states of ^{13}C. The second stage uses this interaction in a coupled-channel calculation, with each channel corresponding to a pair of ^{24}Mg, ^{13}C states. We have also included the orientation dependence associated with the spin-orbit term in the ^{24}Mg optical potential, although in this part of the calculation we have not included the ^{24}Mg deformation. The formulae are derived in Sec. II, the results of the calculation are compared with experimental data in Sec. III, and our conclusions are given in Sec. IV.

II. THE FORMALISM

A. Spin independent potentials

The ^{24}Mg target is assumed to be an axially-symmetric deformed nucleus. We are concerned here only with its orientation degrees of freedom (α,β), and with the $K=0$ rotational band

$$\Phi^{I_c}_{M_c}(\alpha,\beta)=\left[\frac{2I_c+1}{4\pi}\right]^{1/2} D^{I_c *}_{M_c,0}(\alpha,\beta,0)$$

$$=i^{-I_c}Y^{I_c}_{M_c}(\beta,\alpha)$$

$$=\left[\frac{2I_c+1}{4\pi}\right]^{1/2} e^{iM_c\alpha}\sum_n (-1)^n \frac{I_c![(I_c-M_c)!(I_c+M_c)!]^{1/2}}{n!(I_c+M_c-n)!(I_c-n)!(n-M_c)!}\left[\cos\frac{\beta}{2}\right]^{2I_c+M_c-2n}\left[\sin\frac{\beta}{2}\right]^{2n-M_c}. \tag{1}$$

The optical potential produced by this nucleus is of the form

$$U(\vec{r},\alpha,\beta)=\sum_{j=0,2,\ldots,} V_j(r)\sum_\mu D^j_{\mu,0}(\alpha,\beta,0)Y^j_\mu(\hat{r})$$

$$=\sum_{j=0,2,\ldots,} V_j(r)i^j\left[\frac{4\pi}{2j+1}\right]^{1/2}\sum_\mu Y^{j*}_\mu(\beta,\alpha)Y^j_\mu(\hat{r}), \tag{2}$$

where $\hat{r}$ is a unit vector in the direction of $\vec{r}$.

The states of ^{13}C are assumed to be adequately described by the spherical shell model. Here the degrees of freedom are the positions, spin, and isospin components of the 13 nucleons,

$$\phi^{s_c}_{m_c} = \phi^{s_c}_{m_c}(\vec{q}_1\sigma_1\tau_1, \ldots, \vec{q}_{13}\sigma_{13}\tau_{13}) , \tag{3}$$

where $\vec{q}_i$ locates the ith nucleon relative to the mass center of ^{13}C (see Fig. 2). The vector $\vec{R}$ locates the mass center of ^{13}C relative to that of ^{24}Mg, so that

$$\vec{r}_i = \vec{R} + \vec{q}_i \quad (i = 1,2, \ldots, 13) . \tag{4}$$

Each of these 13 nucleons feels the ^{24}Mg optical potential (2). Using this interaction, the matrix elements needed for a coupled-channel analysis of the inelastic scattering in the ^{13}C and ^{24}Mg system may be written

$$F^J_{cc'}(R) = \langle [\Phi^{I_c}(\alpha,\beta)[Y^{l_c}(\hat{R})\phi^{s_c}(\vec{q}\sigma\tau)]^{j_c}]^J_M \mid \sum_{i=1}^{13} U(\vec{r}_i,\alpha,\beta) \mid [\Phi^{I_{c'}}(\alpha,\beta)[Y^{l_{c'}}(\hat{R})\phi^{s_{c'}}(\vec{q}\sigma\tau)]^{j_{c'}}]^J_M \rangle_R . \tag{5}$$

Evaluation of this matrix element requires summation and integration over the variables $\vec{q}_i$, σ_i, τ_i, α, β, and $\hat{R}$, while the magnitude R is kept constant.

If we substitute (1), (2), and (3) into (5) and do some straightforward angular momentum recoupling, we get

$$F^J_{cc'}(R) = (-1)^{I_c+2J}\left[\frac{(2l_c+1)(2l_{c'}+1)(2I_c+1)(2I_{c'}+1)}{4\pi(2J+1)}\right]^{1/2}$$
$$\times \sum_{l,s,j} \frac{(-1)^{2j} i^{l_c+l_{c'}-l}}{[(2l+1)(2j+1)^2]^{1/2}} ((I_c j_c)_J (I_{c'} j_{c'})_J \mid (I_c I_{c'})_j (j_c j_{c'})_j)_0$$
$$\times ((l_c s_c)_{j_c} (l_{c'} s_{c'})_{j_{c'}} \mid (l_c l_{c'})_l (s_c s_{c'})_s)_j (l_c l_{c'} 00 \mid l0)(I_c I_{c'} 00 \mid j0) M_{lsj}(R) , \tag{6a}$$

where

$$M_{lsj}(R) = \sum_{\sigma\tau} \int d\hat{R}\, d\vec{q}_1 \cdots d\vec{q}_{13} \left[\{ Y^l(\hat{R})[\phi^{s_c}(\vec{q}\sigma\tau)\phi^{s_{c'}}(\vec{q}\sigma\tau)]^s \}^j \sum_{i=1}^{13} V_j(r_i) Y^j(\hat{r}_i) \right]_0 . \tag{6b}$$

The 9-j recoupling amplitudes are used in an obvious manner in (6a) to rearrange the factors in (5) to enable us to make use of the well-known theorem

$$[Y^{k_1}(\hat{a}) Y^{k_2}(\hat{a})]^k_m = i^{k_1+k_2-k} \left[\frac{(2k_1+1)(2k_2+1)}{4\pi(2k+1)}\right]^{1/2} (k_1 k_2 00 \mid k0) Y^k_m(\hat{a}) . \tag{6c}$$

The evaluation of the integral in (6b) requires us to express the $\vec{r}_i$-dependent quantities in terms of $\vec{R}$ and $\vec{q}_i$. To this end, we define functions $g^j_{l,s}(R,q)$ by

$$V_j(r) Y^j_m(\hat{r}) = \sum_{l,s} g^j_{l,s}(R,q)[Y^l(\hat{R}) Y^s(\hat{q})]^j_m , \tag{7}$$

where $\vec{r}$, $\vec{R}$, and $\vec{q}$ are related by (4). Then $\hat{R}$ in (6b) can be integrated to yield an R-dependent single-particle matrix element

$$M_{lsj}(R) = \left[\frac{2j+1}{2s+1}\right]^{1/2} \sum_{\sigma\tau} \int d\vec{q}_1 \cdots d\vec{q}_{13} \left\{ [\phi^{s_c}(\vec{q}\sigma\tau)\phi^{s_{c'}}(\vec{q}\sigma\tau)]^s \sum_{i=1}^{13} g^j_{ls}(R,q_i) Y^s(\hat{q}_1) \right\}_0$$
$$= (-1)^{s+s_{c'}+s_c} \left[\frac{(2s_c+1)(2j+1)}{2s+1}\right]^{1/2} \left\langle \phi^{s_c}_m \left| \sum_{i=1}^{13} g^j_{ls}(R,q_i)[Y^s(\hat{q}_i)\phi^{s_{c'}}]^{s_c}_m \right\rangle . \tag{8}$$

Since we have assumed that the ^{13}C wave functions $\phi^{s_c}_m$, $\phi^{s_{c'}}_{m'}$ are shell-model states, the single-particle matrix element (8) can be evaluated using standard fractional parentage techniques.

We include in our calculation only the $I_c=0$ and 2 states of the ^{24}Mg $K=0$ rotational band. Then the only values of j that contribute to $F(R)$ in (6a) are $j=0$, 2, and 4. We take for $U(\vec{r},0,0)$ in (2) a Woods-Saxon potential with a quadrupole deformation,

$$U(\vec{r},0,0)=\frac{V_0}{1+\exp([r-R_0\{1+\beta Y_0^2(\theta,0)\}]/a)} \tag{9a}$$

from which the $V_j(r)$ needed in (2) can be calculated by

$$V_j(r)=2\pi\int_{\vartheta=0}^{\pi}\sin\vartheta\,d\theta\frac{Y_0^{j*}(\vartheta,0)}{1+\exp([r-R_0\{1+\beta Y_0^2(\theta,0)\}]/a)}\ . \tag{9b}$$

If we were to evaluate (9b) using an expansion in β up to first order, then only $j=0$ and 2 would be nonzero. In fact, we do not use an expansion in β but we integrate (9b) numerically. However, we neglect the $j=4$ contribution. This will introduce some error in the calculation of the ($I_c=2$) to ($I_{c'}=2$) reorientation terms, but this should have little effect on the spin flip probability.[6]

Equation (9a) gives the method of deforming the nuclear part of the optical potential. To obtain a deformed Coulomb potential, we assume that the charge density ρ of ^{24}Mg is constant within a surface given by

$$R(\beta,\theta)=R_0[1+\beta Y_0^2(\vartheta,0)]$$

and equal to

$$12e/(\tfrac{4}{3}\pi R_0^3)\ .$$

This yields the following Coulomb potential energy function, to first order in β:

$$U_{\text{Coul}}(\vec{r},0)=12e^2\left[\frac{1}{r}+\tfrac{3}{5}\beta\frac{R_0^2}{r^3}Y_0^2(\hat{r})\right]\quad r>R_0 \tag{10a}$$

$$=12e^2\left[\frac{3R_0^2-r^2}{2R_0^3}+\tfrac{3}{5}\beta\frac{r^2}{R_0^3}Y_0^2(\hat{r})\right]\quad r<R_0\ , \tag{10b}$$

which determines $V_0(r)$ and $V_2(r)$ for the Coulomb part of the optical potential.

It only remains to calculate the $g^j_{l,s}(R,q)$ defined by (7). For $j=0$ this is essentially a Slater expansion,

$$\frac{1}{\sqrt{4\pi}}V_0(r)=\frac{1}{\sqrt{4\pi}}V_0(|\vec{R}+\vec{q}|)$$

$$=\sum_l g^0_{l,l}(R,q)[Y^l(\hat{R})Y^l(\hat{q})]^0_0$$

$$=\frac{1}{4\pi}\sum_l(2l+1)^{1/2}g^0_{l,l}(R,q)P_l(\hat{R}\cdot\hat{q})\ , \tag{11a}$$

from which we can project $g^0_{l,l}(R,q)$ by a single integration

$$g^0_{l,l}(R,q)=[\pi(2l+1)]^{1/2}\int_{x=-1}^{1}V_0[(R^2+q^2+2Rqx)^{1/2}]P_l(x)dx\ . \tag{11b}$$

To get the $j\neq0$ terms in (7) we rewrite the left-hand side in terms of a solid harmonic.

$$V_j(r)Y^j_m(\hat{r})=\frac{V_j(|\vec{R}+\vec{q}|)}{|\vec{R}+\vec{q}|^j}\mathscr{Y}^j_m(\vec{R}+\vec{q})\ . \tag{12}$$

The solid harmonic can be decomposed using

$$\mathscr{Y}^j_m(\vec{R}+\vec{q})=\sum_{p=0}^{j}\left[\frac{4\pi(2j+1)!}{(2p+1)!(2[j-p]+1)!}\right]^{1/2}[\mathscr{Y}^p(\vec{R})\mathscr{Y}^{j-p}(\vec{q})]^j_m\ , \tag{13a}$$

which can be derived by applying the binomial expansion to

$$\mathscr{Y}^j_j(\vec{R}+\vec{q})=\frac{(-i)^j}{2^j j!}\left[\frac{(2j+1)!}{4\pi}\right]^{1/2}(R_x+iR_y+q_x+iq_y)^j\,. \tag{13b}$$

The factor

$$V_j(|\vec{R}+\vec{q}|)/|\vec{R}+\vec{q}|^j$$

can be expanded as in (11),

$$\frac{V_j(|\vec{R}+\vec{q}|)}{|\vec{R}+\vec{q}|^j}=\sum_{l'}(2l'+1)^{1/2}f_{l'}(R,q)[Y^{l'}(\hat{R})Y^{l'}(\hat{q})]^0_0\,, \tag{14a}$$

$$f_{l'}(R,q)=2\pi\int_{x=-1}^{1}\frac{V_j[(R^2+q^2+2Rqx)^{1/2}]}{[R^2+q^2+2Rqx]^{j/2}}P_{l'}(x)dx\,, \tag{14b}$$

so that (12) becomes the double sum

$$V_j(r)Y^j_m(\hat{r})=\sum_{l',p}\left[\frac{4\pi(2j+1)!}{(2p+1)!(2[j-p]+1)!}\right]^{1/2}f_{l'}(R,q)R^pq^{j-p}[Y^{l'}(\hat{R})Y^{l'}(\hat{q})]^0_0[Y^p(\hat{R})Y^{j-p}(\hat{q})]^0_0\,. \tag{15a}$$

By recoupling the four spherical harmonics and using (6c), this can be rewritten as

$$\begin{aligned}V_j(r)Y^j_m(\hat{r})=&\sum_{l,s}[Y^l(\hat{R})Y^s(\hat{q})]^j_m i^{j-l+s}\\&\times\sum_{\substack{p=0,1,\ldots,j\\ l'}}(-1)^pR^pq^{j-p}f_{l'}(R,q)\\&\times\left[\frac{(2j)!(2l+1)(2s+1)}{(2p)!(2[j-p])!(2l'+1)!4\pi}\right]^{1/2}U(lsp[j-p];jl')(lp00\,|\,l'0)(s[j-p]00\,|\,l'0)\,,\end{aligned} \tag{15b}$$

from which we can extract the $g^j_{l,s}(R,q)$ of (7).

For the wave functions $\phi^{s_c}_m$ of the low-lying states of ^{13}C shown in Fig. 1, we choose simple configurations, which are nevertheless a reasonable approximation.[11] We take the configuration

$$(1s_{1/2})^4(1p_{3/2})^8(nlj)^1$$

with $nlj=1p_{1/2}$ for the ground state, $2s_{1/2}$ for the 3.09 MeV level, $1d_{5/2}$ for the 3.85 MeV level, and $1d_{3/2}$ for the 8.2 MeV level. We also consider the 3.68 MeV $\frac{3}{2}^-$ level which we take to be

$$[(1s_{1/2})^4[1p_{3/2}{}^7 1p_{1/2}]^{J=2,T=0}1p_{1/2}]^{s_c=3/2}_m\,.$$

Using these wave functions it is straightforward to evaluate the angular part of Eq. (8). The radial part was computed with single-particle wave functions generated in a Woods-Saxon well with radius parameter $r_0=1.25$ fm and diffuseness $a=0.65$ fm. As usual the well depth was fitted to the separation energies 11.12, 4.95, 1.09, and 1.86 MeV for the $1p_{3/2}$, $1p_{1/2}$, $1d_{5/2}$, and $2s_{1/2}$ states, respectively. Note that the $1d_{3/2}$ level is unbound so we used the same separation energy as in the $1d_{5/2}$ case.

In the harmonic oscillator shell model of ^{13}C, the $(1s_{1/2})^4(1p_{3/2})^8 1d_{5/2}$ configuration has no quanta of center-of-mass motion. However, the $2s_{1/2}$ and $1d_{3/2}$ states have, respectively, 5.1% and 12.8% of components with one quantum of center-of-mass motion. We have not eliminated these spurious components from our calculation.

B. Spin-dependent potentials

In the previous derivation, the origin of the torque exerted on the ^{13}C was the deformation of the central part of the ^{24}Mg optical potential. However, even a spherical optical potential can exert a torque if it has a noncentral part, such as a spin-orbit term $U_{so}(r)\vec{l}_r\cdot\vec{s}$. We now consider the contribution of a spherical spin-orbit

term to the channel-coupling form factor (5).

Let $\vec{p}_{r_i}$ and $\vec{p}_{q_i}$ be the linear momenta of the ith nucleon relative to the mass centers of ^{24}Mg and ^{13}C, respectively, and let $\vec{p}_{\vec{R}}$ be the total momentum of ^{13}C, relative to the mass center of ^{24}Mg. Then (4) implies that

$$\begin{aligned}\vec{p}_{\vec{r}_i}&=\tfrac{1}{13}\vec{p}_{\vec{R}}+\vec{p}_{\vec{q}_i}\ ,\\ \vec{l}_{\vec{r}_i}&=\vec{r}_i\times\vec{p}_{\vec{r}_i}=(\vec{R}+\vec{q}_i)\times(\tfrac{1}{13}\vec{p}_{\vec{R}}+\vec{p}_{\vec{q}_i})\\ &=\tfrac{1}{13}\vec{R}\times\vec{p}_{\vec{R}}+\tfrac{1}{13}\vec{q}_i\times\vec{p}_{\vec{R}}+\vec{R}\times\vec{p}_{\vec{q}_i}+\vec{q}_i\times\vec{p}_{\vec{q}_i}\ ,\end{aligned}\tag{16}$$

in which we have neglected center of mass recoil corrections. Then the spin-orbit contribution to the ^{24}Mg optical potential is

$$\sum_i U_{\rm so}(r_i)\vec{l}_{\vec{r}_i}\cdot\vec{s}_i=\sum_{i=1}^{13}U_{\rm so}(|\vec{R}+\vec{q}_i|)[\tfrac{1}{13}\vec{R}\times\vec{p}_{\vec{R}}+\tfrac{1}{13}\vec{q}_i\times\vec{p}_{\vec{R}}+\vec{R}\times\vec{p}_{\vec{q}_i}+\vec{q}_i\times\vec{p}_{\vec{q}_i}]\cdot\vec{s}_i\ .\tag{17a}$$

The first term in this sum,

$$\tfrac{1}{3}\sum_{i=1}^{13}U_{\rm so}(|\vec{R}+\vec{q}_i|)\vec{L}_{\vec{R}}\cdot\vec{s}_i\tag{17b}$$

has the general structure of a spin-orbit interaction for the relative vector $\vec{R}$ and can be evaluated in a straightforward manner. Thus

$$\begin{aligned}F_{\rm so}(R)&=\langle[\Phi^{I_c}(\alpha,\beta)[Y^{l_c}(\hat{R})\phi^{s_c}(\vec{q}\sigma\tau)]^{j_c}]^J_M\,|\\ &\quad\times\tfrac{1}{13}\sum_{i=1}^{13}U_{\rm so}(|\vec{R}+\vec{q}_i|)\vec{L}_{\vec{R}}\cdot\vec{s}_i\,|\,[\Phi^{I_{c'}}(\alpha,\beta)[Y^{l_{c'}}(\hat{R})\phi^{s_{c'}}(\vec{q}\sigma\tau)]^{j_{c'}}]^J_M\rangle\\ &=\delta_{I_c,I_{c'}}\delta_{j_c,j_{c'}}\langle[Y^{l_c}(\hat{R})\phi^{s_c}(\vec{q}\sigma\tau)]^{j_c}_m\,|\,\tfrac{1}{13}\sum_{i=1}^{13}U_{\rm so}(|\vec{R}+\vec{q}_i|)\vec{L}_{\vec{R}}\cdot\vec{s}_i\,|\,[Y^{l_{c'}}(\hat{R})\phi^{s_{c'}}(\vec{q}\sigma\tau)]^{j_c}_m\rangle\ .\end{aligned}\tag{18}$$

The spin-orbit interaction is unable to couple different rotational states of ^{24}Mg because we have ignored its deformation. Next, we perform a Slater expansion on $U_{\rm so}$,

$$U_{\rm so}(|\vec{R}+\vec{q}|)=\sum_l[(2l+1)]^{1/2}h_l(R,q)[Y^l(\hat{R})Y^l(\hat{q})]^0_0\ .\tag{19}$$

If we use (6c) and the reduced matrix element of $\vec{L}_{\vec{R}}$,

$$\langle Y^{l_c}_m(\hat{R})\,|\,[L_{\vec{R}}Y^{l_{c'}}(\hat{R})]^{l_c}_m\rangle=-\hbar\delta_{l_c,l_{c'}}[l_c(l_c+1)]^{1/2}\ ,$$

we can show that (18) is equal to

$$\begin{aligned}F_{\rm so}(R)=&\frac{\hbar}{13}\delta_{I_c,I_{c'}}\delta_{j_c,j_{c'}}\left[\frac{l_{c'}(l_{c'}+1)}{4\pi}\right]^{1/2}\\ &\times\sum_{l,p}i^{l+l_{c'}-l_c}(2l+1)^{1/2}(ll_{c'}00\,|\,l_c0)U(ps_{c'}l_cj_c;s_cl_{c'})U(l1l_cl_{c'};pl_{c'})\\ &\times\langle\phi^{s_c}_m\Big|\sum_{i=1}^{13}h_l(R,q_i)\{[Y^l(\hat{q}_i)s^1]^p\phi^{s_{c'}}\}^{s_c}_m\rangle\ .\end{aligned}\tag{20}$$

If $\phi^{s_c}_m$ and $\phi^{s_{c'}}_{m'}$ are single-particle states beyond a ^{12}C closed core, then the reduced matrix element in (20) can be shown to be equal to

$$\langle \phi_{m_1}^{n_1 l_1 j_1} \mid h_l(R,q)\{[Y^l(\hat{q})s^1]^p \phi^{n_2 l_2 j_2}\}_{m_1}^{j_1} \rangle$$
$$= i^{l+l_2-l_1}\hbar \left[\frac{(2l+1)(2j_2+1)}{4\pi(2j_1+1)}\right]^{1/2}$$
$$\times \int_0^\infty u_{n_1 l_1 j_1}(q) u_{n_2 l_2 j_2}(q) h_l(R,q) q^2 dq$$
$$\times \left[\frac{(-1)^{j_2-(1/2)-l_2}}{\sqrt{2}}(pj_2-1\tfrac{1}{2} \mid j_1-\tfrac{1}{2})(l\,10-1 \mid p-1)-\tfrac{1}{2}(pj_2 0-\tfrac{1}{2} \mid j_1-\tfrac{1}{2})(l\,100 \mid p0)\right] . \quad (21)$$

The angular part of this expression can most easily be derived by noting that $\{[Y^l(\hat{q})s^1]^p \phi^{n_2 l_2 j_2}\}_{m_1}^{j_1}$ and $\phi_{m_1}^{n_1 l_1 j_1}$ are proportional, with a proportionality factor independent of $\hat{q}$ and m_1. This factor can be obtained by calculating the ratio of these two quantities for $\hat{q}=\hat{z}$ and $m=-\frac{1}{2}$.

The remaining three terms in Eq. (17a) are difficult to deal with in general. We neglect them except in the cases where $s_c = s_{c'} = \frac{1}{2}^-$ or $\frac{1}{2}^+$ since these are clearly most important for the spin flip probability. In these cases the third and fourth terms of Eq. (17a) will not lead to spin flip and are neglected. The second term, however, will produce spin flip and gives a contribution involving $\vec{L}_{\vec{R}}$. This term can be taken into account by replacing $h_0(R,q_i)$ in Eq. (20) by

$$h_0(R,q_i)+\frac{3q_i}{R}h_1(R,q_i)$$

for the $\frac{1}{2}^-$ case and by

$$h_0(R,q_i)+\frac{q_i}{R}h_1(R,q_i)$$

for the $\frac{1}{2}^+$ case. This replacement for the $\frac{1}{2}^-$ case produces a significant reduction in the form factor and the resulting spin flip probability.

It should be noted that (20) and (21) yield an expression for $F_{so}(R)$ which is unsymmetric with respect to exchange of c and c'. This asymmetry arises because we have only retained one (non-Hermitian) term (17b) of a full (Hermitian) expression (17a). If the coupled-channel calculation using $F_{so}(R)$ is to yield a unitary S matrix, then $F_{so}(R)$ must be Hermitian. Thus in the calculation whose result is presented in the next section, we have replaced (20) and (21) by an expression symmetrized with respect to c and c'. This is equivalent to using the interaction

$$\frac{1}{26}\sum_{i=1}^{13}\{U_{so}(\mid \vec{R}+\vec{q}_i \mid)\vec{L}_{\vec{R}}+\vec{L}_{\vec{R}}U_{so}(\mid \vec{R}+\vec{q}_i \mid)\}\cdot\vec{s}_i \quad (22)$$

instead of (17b).

III. CALCULATION AND RESULTS

A. Spin-independent potentials

Our main interest here is in the probability P_1 that the excitation of the 1.37 MeV 2^+ level of ^{24}Mg is accompanied by a change in the sign of the component of the ^{13}C $\frac{1}{2}^-$ ground state spin perpendicular to the reaction plane (or equivalently the component of the ^{24}Mg spin is ± 1).

In this section we shall use spin-independent potentials so that the spin-flip probability P_1 arises entirely from the inelastic excitation of the levels of ^{13}C shown in Fig. 1. As explained in Sec. II, we generated form factors for inelastic excitation by the single folding of a deformed nucleon-^{24}Mg potential. For this purpose we used the Becchetti-Greenlees potential[12] listed in Table I; the spin-dependent parts of this potential are to be ignored for present purposes. One could also use the folded potentials to describe the elastic scattering in a given state of the ^{13}C+^{24}Mg system. However, in order to minimize uncertainties we decided to use the form factor from our previous phenomenological analysis,[6] i.e., the scalar part of the deformed optical model potential listed in Table I. We have not included reorienta-

TABLE I. Optical model parameters.

	V (MeV)	r_R (fm)	a_R (fm)	W_v (MeV)	r_I (fm)	a_I (fm)	V_{so} (MeV)	r_{so} (fm)	a_{so} (fm)	r_c (fm)	β_2
Nucleon-^{24}Mg	50.0	1.17	0.75				6.2	1.01	0.75		0.40
^{13}C-^{24}Mg	40.0	1.165	0.658	19.1	1.165	0.658				1.165	0.33

tion terms, i.e., nonscalar terms, in the elastic scattering since the reorientation of ^{24}Mg was found[6] to produce a negligible effect on the spin-flip probability and the reorientation of ^{13}C can only enter when the spin s is greater than $\frac{1}{2}$. The strengths of the Coulomb form factors for inelastic excitation were taken from the electromagnetic data.[13]

Using these form factors we have carried out a series of coupled channel calculations including various combinations of the levels shown in Fig. 1. The extraction of P_1 from the reaction amplitudes was discussed in Ref. 6. Most of the calculations were carried out with the code INCH, but we made a few calculations with the code CHORK (Ref. 14) and, after some effort, obtained agreement between the results for the spin-flip probability.

For brevity we shall use the notation (s_c,I_c) in which s_c denotes the spin of the ^{13}C projectile and I_c the spin of the ^{24}Mg target. Thus, our calculations always included the $(\frac{1}{2}^-,0^+)$ and $(\frac{1}{2}^-,2^+)$ levels, i.e., ^{13}C in its ground state with ^{24}Mg in the ground and first excited 2^+ state. Various additional (s_c,I_c) combinations were considered which produce a nonzero spin-flip probability. These additional combinations did not significantly affect the cross sections for $(\frac{1}{2}^-,0^+)$ elastic scattering and $(\frac{1}{2}^-,2^+)$ target inelastic scattering. Our predictions are compared with the data in Fig. 3. Note that we have scaled the deformation of the potential which was used to generate the inelastic form factors so that the magnitude of the $(\frac{1}{2}^-,2^+)$ cross section is approximately correct. The predicted shape is reasonable, in fact a little better than obtained phenomenologically in Ref. 6, although the fit to the $(\frac{1}{2}^-,0^+)$ elastic cross section is poorer. The probability P_0 of populating the ^{24}Mg 2^+ level with component $K'=0$ perpendicular to the reaction plane was measured[3] to be $4.2\pm5.5\%$ and[4] $32.2\pm3.5\%$. Our calculations give 41.7%, in fair agreement with the latter value. We have not tried to vary the potentials to maximize the agreement with the data since this is not expected to have a significant effect on the spin-flip probabilities.[6]

In Fig. 4 the dashed curve gives the spin-flip probability P_1 obtained by including, in addition to the standard $(\frac{1}{2}^-,0^+)$ and $(\frac{1}{2}^-,2^+)$ levels, the $(\frac{1}{2}^+,0^+)$ combination. The dotted curve results from including the $(\frac{1}{2}^+,2^+)$ combination instead, and it is comparable to the dashed curve. The spin-flip probability is considerably enhanced by coherently summing the amplitudes for the two cases as indicated at three angles by the crosses. However, this procedure underestimates the true result (full line) obtained by including both the $(\frac{1}{2}^+,0^+)$ and $(\frac{1}{2}^+,2^+)$ in a coupled-channel calculation. Thus it is important to couple both the 0^+ and 2^+ states of ^{24}Mg with the various levels of ^{13}C.

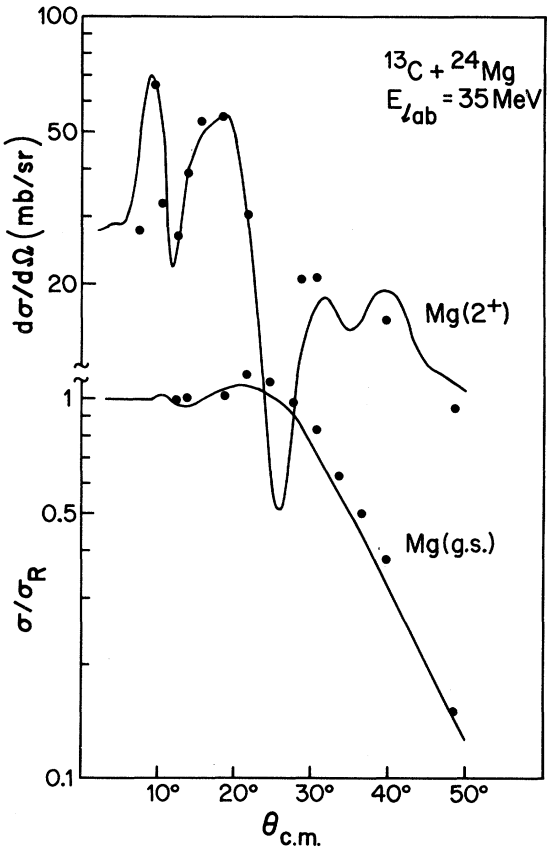

FIG. 3. Comparison of coupled channel cross sections for elastic scattering and inelastic excitation of the 1.37 MeV 2^+ level of ^{24}Mg with the data of Ref. 3.

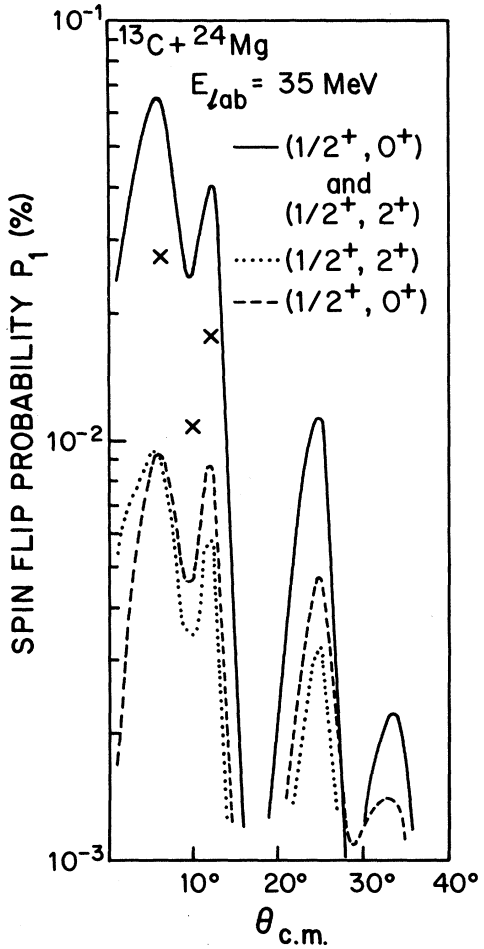

FIG. 4. Spin flip probability P_1 obtained by including different combinations of the $(\frac{1}{2}^+,0^+)$ and $(\frac{1}{2}^+,2^+)$ levels in coupled channel calculations. The crosses indicate an approximation to the full curve; see text.

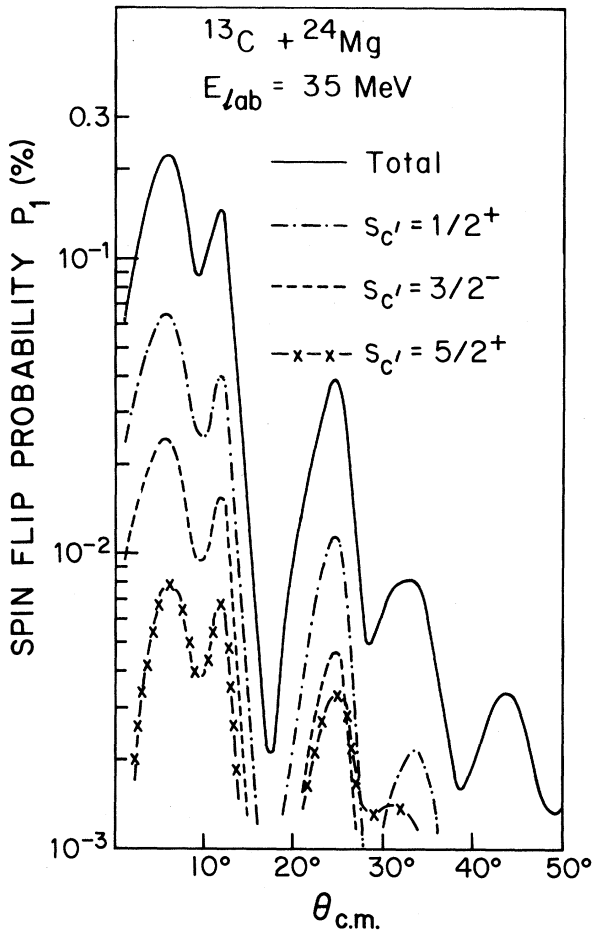

FIG. 5. Spin flip probabilities P_1 obtained by including various levels in ^{13}C. The full curve shows the estimated total result.

We have tested whether in the calculations of Fig. 4 processes of the type $(\frac{1}{2}^-,I_c)\rightarrow(\frac{1}{2}^+,I_c)\rightarrow(\frac{1}{2}^-,I_c)$ dominate since they could be incorporated into an effective elastic optical potential which is spin dependent. This does not appear to be valid in general.

We have carried out a series of calculations in which we include the $(\frac{1}{2}^-,0^+)$, $(\frac{1}{2}^-,2^+)$, $(s_{c'},0^+)$, and $(s_{c'},2^+)$ levels, where $s_{c'}$ is $\frac{1}{2}^+$, $\frac{3}{2}^-$, or $\frac{3}{2}^+$. For the case where $s_{c'}=\frac{5}{2}^+$, we could only include the $(\frac{5}{2}^+,0^+)$ case because of the very large number of channels generated by the $(\frac{5}{2}^+,2^+)$ combination. The resulting spin-flip probabilities for the $s_{c'}=\frac{1}{2}^+$, $\frac{3}{2}^-$, and $\frac{5}{2}^+$ calculations are shown in Fig. 5. Clearly the shapes of the curves are quite similar, but the magnitudes depend strongly on $s_{c'}$ with the $\frac{1}{2}^+$ case producing the largest result. The $\frac{3}{2}^+$ case is not illustrated since the spin-flip probability at the 6° peak is only 3×10^{-4}%. Thus the effect of the 8.2 MeV $\frac{3}{2}^+$ level in ^{13}C is negligible. This is due to the large negative Q value for this state, which brings the c.m. energy close to the Coulomb barrier. If the magnitude of the Q value is artificially reduced the predictions become comparable to the $\frac{5}{2}^+$ case.

In order to estimate the total effect we coherently add the spin-flip amplitudes obtained for the various $s_{c'}$ values; this leads to the full curve of Fig. 5. The value of the spin flip probability P_1 at 10° is approximately 0.1% which is about an order of magnitude less than the observed value (1.67±0.52 % in Ref. 3 and 1.0±0.5 % in Ref. 4). It should be noted that our full curve represents an approximation, albeit unavoidable, since we have simply added the amplitudes from the separate calculations for the various $s_{c'}$ values. We have carried out a few coupled channel calculations with various level combinations in

order to try to assess the accuracy of this approximation. We found it to be very accurate if the coupling between states with different $s_{c'}$ is neglected. If these couplings are included the approximation deteriorates, although it is more accurate in this instance than in the discussion associated with Fig. 4.

We suggest that the full curve of Fig. 5 is uncertain by a factor of ≈ 2, which is certainly tolerable within the context of the present exploratory calculations. Finally, we believe it is significant that the $s_{c'}=\frac{1}{2}^+$, $\frac{3}{2}^-$, and $\frac{5}{2}^+$ contributions all interfere constructively, whereas the $s_{c'}=\frac{3}{2}^+$ contribution is destructive since only in the latter case do we have a matrix element between a $p_{1/2}$ and a $j=l-\frac{1}{2}$ orbital. Of course the effect is numerically insignificant with the present bombarding energy.

B. Spin-dependent potentials

We now include spin-dependent terms in the potentials as explained in Sec. II B. In Fig. 6 the dashed curve gives the spin flip probability from a two-level calculation which includes just the $(\frac{1}{2}^-,0^+)$ and $(\frac{1}{2}^-,2^+)$ levels. In our approximation the inelastic coupling between the 0^+ and 2^+ levels is the same as in Sec. III A, so the spin flip arises from the spin-orbit contribution to the elastic scattering in the 0^+ and 2^+ states. Our values for P_1 in the two level case are estimated to be about a factor of 4 larger than would be obtained with the double-folding results of Petrovich *et al.*[7] We have repeated the calculations of Fig. 5 including spin-dependent potentials, *except* for elastic scattering in the $(\frac{1}{2}^-,0^+)$ and $(\frac{1}{2}^-,2^+)$ levels because this would lead to double counting when we sum the spin-flip amplitudes. A sample result is shown by the dotted-dashed curve in Fig. 6, which corresponds to the case $s_{c'}=\frac{1}{2}^+$. In this case it is found that P_1 is enhanced compared to the previous result in Fig. 5. Now by adding the spin flip amplitudes for the different calculations and the two level calculation, we obtain the full curve in Fig. 6. By way of commenting on the accuracy of this approach, we note that if the spin flip amplitudes corresponding to the dashed and dotted-dashed curves of Fig. 6 are added, the resulting values of P_1 are very close to those obtained in a calculation with the $(\frac{1}{2}^-,0^+)$, $(\frac{1}{2}^-,2^+)$, $(\frac{1}{2}^+,0^+)$, and $(\frac{1}{2}^+,2^+)$ levels which includes all spin-dependent terms.

It is clear that P_1 has only been slightly increased from the previous results in Sec. III A. The 6° peak of P_1 now has the value 0.3% compared to the previous 0.2%. At 10° we still obtain $\approx 0.1\%$ for P_1, whereas the experiments[3,4] are consistent with 1% at this angle.

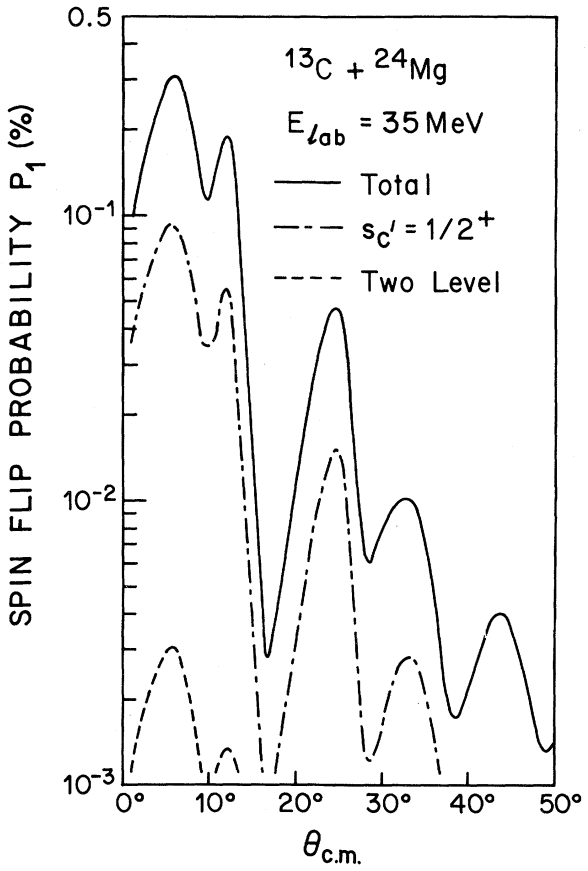

FIG. 6. Spin flip probabilities when spin-dependent potentials are included. The dashed curve corresponds to a calculation with the $(\frac{1}{2}^-,0^+)$ and $(\frac{1}{2}^-,2^+)$ levels. The dotted-dashed curve allows for the excitation of the $s_{c'}=\frac{1}{2}^+$ state and the full curve shows our estimated total result; see text for a precise description.

C. Predictions for excited states of ^{13}C

As far as we are aware, no data exist for $^{13}C+^{24}Mg$ where ^{13}C is left in an excited state. Nevertheless we feel that it is worthwhile to discuss our predictions, particularly regarding the polarization. As a fairly representative case we display in Fig. 7 the $(\frac{1}{2}^+,0^+)$ and $(\frac{1}{2}^+,2^+)$ cross sections predicted by a coupled channel calculation which included these combinations along with the $(\frac{1}{2}^-,0^+)$ and $(\frac{1}{2}^-,2^+)$ levels. As in Sec. III A spin-dependent terms were omitted from the potentials. If they are included the main change in the results is an enhancement in the ejectile polarization. Both the $(\frac{1}{2}^+,0^+)$ and $(\frac{1}{2}^+,2^+)$ cross sections are ~ 1 mb/sr at very forward angles, with the $(\frac{1}{2}^+,2^+)$ cross section falling off more rapidly as a function of angle.

More interesting, however, is the large magnitude of the polarizations predicted (the vector polarization perpendicular to the reaction plane, i.e., in the direction $\vec{k}_i \times \vec{k}_f$). Similar features were observed for the other excited states of ^{13}C, whereas when ^{13}C is left in its $\frac{1}{2}^-$ ground state the polarization is predicted to be much less than 0.1 in magnitude. The origin of these large polarizations appears to be quite general and model independent, as we now discuss.

First consider the channel coupling matrix elements of Eq. (6a)

$$F^J_{c'c} \propto (l_c l 00 \mid l_{c'} 0) U(I_c j J j_{c'}; I_{c'} j_c) \times ((ss_{c'})_{s_c} (l l_{c'})_{l_c} \mid (sl)_j (s_{c'} l_{c'})_{j'})_{j_c} . \tag{23}$$

Here we have suppressed phases and simply indicated the dependence on the large angular momenta l_c, $l_{c'}$, j_c, and $j_{c'}$; the other angular momenta are small. In general several tensor combinations l, s, and j may contribute to the matrix element and will need to be discussed. Now applying the relations given in the Appendix for the angular momentum coupling coefficients, we have

$$F^J_{c'c} \propto (I_c I_{c'} [J - j_c][j_{c'} - J] \mid j [j_{c'} - j_c])(sl [j_{c'} - j_c + l_c - l_{c'}][l_{c'} - l_c] \mid j [j_{c'} - j_c]) \times (ss_{c'} [j_{c'} - j_c + l_c - l_{c'}][l_{c'} - j_{c'}] \mid s_c [l_c - j_c]) d^l_{l_{c'} - l_c, 0} \left[\frac{\pi}{2} \right] . \tag{24}$$

The reduced rotation matrix, d, vanishes unless $(l + l_{c'} - l_c)$ is even.

In order to appreciate the significance of this result, consider a general reaction amplitude

$$\mathscr{I}''_{K'\mu';K\mu} = \frac{1}{ik_c} \sum_{\substack{j_c l_c \\ j_{c'} l_{c'} \\ J\pi}} (l_c s_c 0\mu \mid j_c \mu)(I_c j_c K\mu \mid J [K + \mu]) \times (l_{c'} s_{c'} \lambda' \mu' \mid j_{c'} [\lambda' + \mu'])(I_{c'} j_{c'} K' [\lambda' + \mu'] \mid J [K + \mu]) \sqrt{4\pi}\, \hat{l}_c Y^{l_{c'}}_{\lambda'}(\theta, 0) \mathscr{M}^{J\pi}_{c'c} . \tag{25}$$

Here c labels the entrance channel, c' labels the exit channel, the quantity $\mathscr{M}$ is the transition matrix between the coupled states, and $\hat{x} = (2x+1)^{1/2}$. The z axis has been chosen in the direction of the entrance channel wave number $\vec{k}_c$ and the y axis in the direction $\vec{k}_c \times \vec{k}_{c'}$. The differential cross section is given by

$$\frac{d\sigma}{d\Omega} = \hat{s}_c^{-2} \hat{I}_c^{-2} \sum_{\substack{K'\mu' \\ K\mu}} |\mathscr{I}''_{K'\mu';K\mu}|^2 . \tag{26}$$

Now if we rotate the coordinate system to one in which the z axis is in the direction $\vec{k}_c \times \vec{k}_{c'}$, i.e., perpendicular to the reaction plane, the reaction amplitude becomes

$$\mathscr{I}^{\perp}_{K'\mu';K\mu} = \sum_{\substack{\bar{\mu}\bar{\mu}' \\ \bar{K}\bar{K}'}} D^{s_c}_{\bar{\mu}\mu} \left[\frac{\pi}{2}, \frac{\pi}{2}, 0 \right] D^{I_c}_{\bar{K}K} \left[\frac{\pi}{2}, \frac{\pi}{2}, 0 \right] D^{s_{c'}*}_{\bar{\mu}'\mu'} \left[\frac{\pi}{2}, \frac{\pi}{2}, 0 \right] D^{I_{c'}*}_{\bar{K}'K'} \left[\frac{\pi}{2}, \frac{\pi}{2}, 0 \right] \mathscr{I}''_{\bar{K}'\bar{\mu}';\bar{K}\bar{\mu}} , \tag{27}$$

where we follow the phase conventions of Rose.[15] Now using the approximate form for the Clebsch-Gordan coefficients of (25) given in the Appendix and the standard asymptotic expression for the spherical harmonic, we easily find

$$\mathscr{I}^{\perp}_{K'\mu';K\mu} = \sum_{\substack{j_c l_c \\ j_{c'} l_{c'} \\ J\pi}} \left[\frac{2l_c}{\pi \sin\theta} \right]^{1/2} \frac{\mathscr{M}^{J\pi}_{c'c}}{k_c} \{ \delta_{\mu, l_c - j_c} \delta_{K, j_c - J} \delta_{\mu', l_{c'} - j_{c'}} \delta_{K', j'_c - J} (-1)^{s_c + j_{c'} - s_{c'} - j_c} e^{-i\{[l_{c'} + (1/2)]\theta + (\pi/4)\}} - \delta_{\mu, j_c - l_c} \delta_{K, J - j_c} \delta_{\mu', j_{c'} - l_{c'}} \delta_{K', J - j_{c'}} (-1)^{I_c + j_c - I_{c'} - j_{c'}} e^{i\{[l_{c'} + (1/2)]\theta + (\pi/4)\}} \} . \tag{28}$$

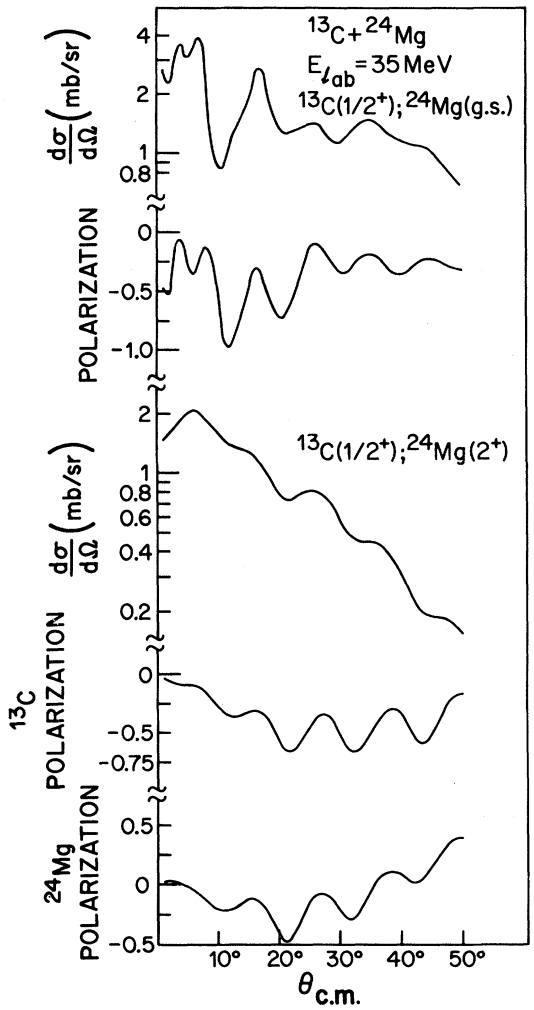

FIG. 7. Cross sections and polarizations for the inelastic scattering of ^{13}C on ^{24}Mg leaving ^{13}C in the 3.09 MeV $\frac{1}{2}^+$ level and ^{24}Mg in the 0^+ ground state or 1.37 MeV 2^+ level.

The first term in the braces corresponds to near side scattering and should dominate. We see that $(l_c - j_c)$ and $(j_c - J)$ can be interpreted as the components of s_c and I_c perpendicular to the reaction plane and similarly for the primed quantities. The second term corresponds to far side scattering and will be smaller; in this case the components of s_c and I_c reverse sign because the orbital angular momentum reverses direction between the two sides of the nucleus. Polarizations obtained with a simple model for $\mathcal{M}$ have been discussed in Ref. 16.

With this interpretation of Eq. (28) we can use Eq. (24) for $V_{c'c}$ to get some idea of the favored components of the spins (perpendicular to the reaction plane). For this purpose we consider a one-step inelastic excitation so that $(s_c, I_c) = (\frac{1}{2}^-, 0^+)$. We first examine the excitation of the $(\frac{1}{2}^+, 0^+)$ pair so that the transferred angular momenta are $l = s = 1$ and $j = 0$. Equation (24) has a maximum magnitude for $j_c - l_c = \pm\frac{1}{2}$ and $j_{c'} - l_{c'} = \mp\frac{1}{2}$ so that $l_c - l_{c'} = \mp 1$. Since the Q value is negative, angular momentum matching favors $l_c - l_{c'}$ positive. Thus, we expect the $j_c - l_c = -\frac{1}{2}$ and $j_{c'} - l_{c'} = +\frac{1}{2}$ components of spin to be preferentially populated, as indicated by the simple vector diagram in Fig. 8(a). This leads to a large negative polarization as shown in Fig. 7. In this case the asymmetry, or vector analyzing power, is of opposite sign and the same magnitude. For general $(s_{c'}, 0^+)$ with $s = s_{c'} + \frac{1}{2}$, the magnitudes are only approximately equal, but the same qualitative arguments apply. The application of Eq. (24) to the excitation of $(s_{c'}, 0^+)$ with $s = s_{c'} - \frac{1}{2}$ is shown in Fig. 8(b). We see that in this case both the polarization and asymmetry are negative. This effect was observed for the excitation of the $(\frac{3}{2}^+, 0^+)$ pair. These cases can be contrasted with the target excitation to the $(\frac{1}{2}^-, 2^+)$ pair for which $s = 0$ and Eq. (24) does not favor any spin direction for the projectile. The polarization is therefore small.

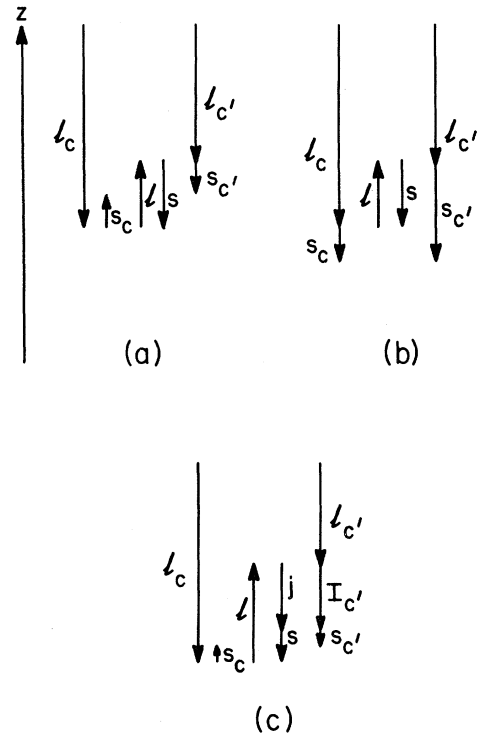

FIG. 8. Schematic vector diagrams indicating, in various cases, the preferred directions of the entrance and exit channel angular momenta and the transferred angular momenta. The z axis is in the direction $\vec{k}_i \times \vec{k}_f$, i.e., perpendicular to the reaction plane.

$(\frac{1}{2}^+, 2^+)$ case. Here the transferred angular momenta l, s, and j may be 1, 1 and 2 or 3, 1 and 2. The latter should be favored since the Q value prefers an angular momentum transfer of 3 units. In this case Eq. (24) favors the orientation given in Fig. 8(c). We thus find a large negative polarization as shown in Fig. 7 and a large positive asymmetry (not illustrated). Figure 7 shows that the polarization of the residual nucleus is predominantly negative as expected, although it is found to change sign at 35°. The population of the 2^+ level with z component ± 1 is not favored by the simple model of Fig. 8(c). The probability P_1 is predicted to have a peak value of 44% and 8° and to fall to less than 10% beyond 15°. Note that in this case Bohr's theorem[17] indicates that the $\frac{1}{2}^-$ projectile and $\frac{1}{2}^+$ ejectile have the same spin component perpendicular to the reaction plane. The same result is given by Eq. (24).

IV. CONCLUSIONS

We have studied the inelastic scattering of ^{13}C on ^{24}Mg, allowing for the excitation of simple shell-model configurations in ^{13}C as well as the rotational 2^+ in ^{24}Mg (see Fig. 1). Our main aim was to calculate the probability P_1 that ^{24}Mg emerges in the 2^+ state with component ± 1 along an axis perpendicular to the reaction plane (and ^{13}C remains in its ground state). Bohr's theorem[17] then ensures that the ^{13}C spin component has flipped sign.

The experiments of Refs. 3 and 4 gave $P_1 = 1.67 \pm 0.52$ and 1.0 ± 0.5 %, respectively, at 10°. These can be compared with our calculated result which was ≈ 0.1% regardless of whether spin dependent potentials were included or not. This value is not negligible in comparison to the data, but it is too small. It should also be pointed out that there are uncertainties in the calculation. Particularly troublesome is the (unavoidable) procedure of adding amplitudes from separate calculations and the approximations with the spin-dependent potentials.

It is worth noting that there is some recent work in a similar vein. Nishioka *et al.*[18] have studied asymmetries for ^{6}Li and ^{7}Li incident on ^{58}Ni. By allowing inelastic excitation of the first excited level in the lithium projectile, they were able to obtain agreement with the data. Imanishi and von Oertzen[19] have studied the ^{12}C+^{13}C system at very low energy, allowing both inelastic excitation of ^{13}C and the transfer of a neutron between the nuclei. They deduce an approximate spin-orbit potential for the entrance channel which is of the same order as required by the data.[5]

Inelastic scattering does play a role of some significance in generating the orientation dependence in heavy ion reactions, but, at least in the present case, this does not appear to be the whole story. Stripping-pickup processes[19,24] can also contribute and we hope to study this effect as well as an improved treatment of the spin-dependent potential at a later date. Any augmentation of the meager data for ^{13}C+^{24}Mg would be highly desirable, as would data bearing on the polarization phenomena we have discussed.

ACKNOWLEDGMENTS

We thank R. C. Johnson for useful comments in connection with Sec. II B. This work was supported in part by the U. S. Department of Energy under Contract No. DE-AC02-79ER10364 and by NATO under Research Grant 224.81.

APPENDIX: ASYMPTOTIC FORMS FOR ANGULAR MOMENTUM RECOUPLING COEFFICIENTS

Brussaard and Tolhoek[20] and Edmonds[21] have given an approximate expression for Clebsch-Gordan coefficients:

$$(Lsm_L m_s \mid Jm_J) \approx d^s_{m_s, J-L}\left[\frac{\pi}{2}\right], \tag{A1}$$

where d is a reduced rotation matrix and we use the definition of Rose.[15] The approximate equality holds when L and J are large, but s is small; also the z component m_J must be small in comparison to J in order that the argument of the reduced rotation matrix can be approximated by $\pi/2$.

One can derive approximate relations for Racah coefficients by expanding in terms of Clebsch-Gordan coefficients, using Eq. (A1) and the standard properties of rotation matrices. The notation throughout is that upper case letters refer to large angular momenta and lower case letters refer to small angular momenta. We obtain for unitary Racah coefficients

$$U(abCD;eF) \approx (ab\,[F-C][D-F] \mid e\,[D-C]) \tag{A2}$$

and

$$U(aBCd;EF) \approx \delta_{B+C,E+F}\,. \tag{A3}$$

Equation (A2) agrees with the result given by Alder *et al.*[22] within a factor of $\hat{X}/\hat{Y}$, where $\hat{\alpha} = (2\alpha+1)^{1/2}$ and X and Y form a triangle with a small angular momentum z. Thus $\hat{X}/\hat{Y}$ is of order

unity. To similar accuracy Eq. (A3) may be obtained from Eq. (A2.2) of Edmonds[21] (or the equivalent formula of Alder *et al.*) by setting his J small in comparison to his J_1 and J_2.

Equation (A3) also follows from Eq. (2.11) of Ponzano and Regge,[23] where it is seen that there is a factor of $(2R)^{-|B+C-E-F|}$, R being of the order of one of the large angular momenta. Thus in Eq. (A3) we have selected only the leading order case. Ponzano and Regge have discussed a geometrical interpretation of a Racah coefficient in terms of a tetrahedron. The condition here that $B+C=E+F$ is the condition that the tetrahedron does not become "hyperflat," i.e., have an imaginary volume, in which case the magnitude of the Racah coefficient is diminished.

Now for unitary 9-j symbols we have expanded in terms of 6-j symbols, used Eqs. (A2) and (A3), and obtained the following results:

$$((ab)_c(dE)_F \mid (ad)_g(bE)_H)_I \approx (ad\,[H-I+F-E][E-F] \mid g\,[H-I]) \times (ab\,[H-I+F-E][E-H] \mid c\,[F-I]) \tag{A4}$$

and

$$((aB)_C(De)_F \mid (aD)_G(Be)_H)_i \approx (-1)^{a+e+i-C-G}\delta_{C+G,B+D}\delta_{C+G,F+H}\,. \tag{A5}$$

Depending on how the 9-j symbol is expanded, Eq. (A4) may be derived by using Eq. (A2) twice together with either Eq. (A3) or the standard properties of Racah and Clebsch-Gordan coefficients. Similarly Eq. (A5) may be derived either by using Eq. (A3) three times or by using Eq. (A2) twice and Eq. (A3) once. Thus the approximations (A2)—(A5) are consistent, which is reasonable since they are all based on Eq. (A1).

In the derivation of Eqs. (A2)—(A5) we have assumed that all the triangle conditions are obeyed, otherwise the Racah coefficient or 9-j symbol vanishes. We have considered those well-known symmetry relations which interchange small angular momenta among themselves and large angular momenta among themselves in Eqs. (A2)—(A5). We find that the symmetry relations are obeyed by our approximate expressions either exactly or to within a factor or factors of the type $\hat{X}/\hat{Y}$, where X and Y form a triangle with a small angular momentum z. Sum rules are also obeyed to similar accuracy provided that the angular momentum summed cannot take both large and small values. Again the same level of accuracy is obtained if one sets one (two) of the small angular momenta to zero in our approximate expressions for Racah coefficients (9-j symbols). Finally we note that the 9-j symbol of Eq. (A4) vanishes if $d=g$, $E=H$, $F=I$, and $(-1)^{a+b+c}=-1$; this condition is embodied in the second Clebsch-Gordan coefficient of our approximate expression.

TABLE II. Comparison of exact and approximate values for 9-j symbols.

x	Y	Exact value	Approximate value
		$((11)_2(222)_{22} \mid (12)_x(122)_Y)_{24}$	
1	23	0.296	0.316
2	22	−0.0416	0
2	23	−0.690	−0.707
3	21	0.00237	0
3	22	0.0627	0
3	23	0.657	0.632
		$((120)_{21}(242)_{22} \mid (124)_Y(202)_{22})_x$	
1	23	1.000	1
2	23	−0.994	−1
2	24	0.0657	0
3	23	0.985	1
3	24	−0.103	0
3	25	0.00410	0

In order to give some indication of the accuracy of these formulae, we compare in Table II the exact values for some arbitrarily chosen unitary 9-j symbols with the approximate results of Eq. (A4) or (A5). It is clear that the accuracy is sufficient for qualitative and semiquantitative discussion.

[1]B. F. Bayman, A. Dudek-Ellis, and P. J. Ellis, Nucl. Phys. A301, 141 (1978).
[2]P. Wust, W. von Oertzen, H. Ossenbrink, H. Lettau, H. G. Bohlen, W. Saathoff, and C. A. Wiedner, Z. Phys. A 291, 151 (1979).
[3]W. Dünnweber, P. D. Bond, C. Chasman, and S. Kubono, Phys. Rev. Lett. 43, 1642 (1979).
[4]D. P. Bybell, D. P. Balamuth, and W. K. Wells, Bull. Am. Phys. Soc. 25, 739 (1980), and private communication.
[5]M. Tanaka, J. Kawa, T. Fukuda, T. Shimoda, K. Katori, S. Nakayama, I. Miura, and H. Ogata, Phys. Lett. 106B, 293 (1981).
[6]Q. K. K. Liu and P. J. Ellis, Phys. Rev. C 22, 540 (1980).
[7]F. Petrovich, D. Stanley, L. A. Parks, and P. Nagel, Phys. Rev. C 17, 1642 (1978).

[8]W. Weiss, P. Egelhof, K. D. Hildebrand, D. Kassen, M. Makowska-Rzeszutka, D. Fick, H. Ebinhaus, E. Steffens, A. Amakawa, and K. I. Kubo, Phys. Lett. 61B, 237 (1976).

[9]P. Egelhof, J. Barrette, P. Braun-Munzinger, W. Dreves, C. K. Gelbke, D. Kassen, E. Steffens, W. Weiss, and D. Fick, Phys. Lett. 84B, 176 (1979).

[10]G. Tungate, R. Böttger, P. Egelhof, K.-H. Möbius, Z. Moroz, E. Steffens, W. Dreves, I. Koenig, and D. Fick, Phys. Lett. 98B, 347 (1981).

[11]M. R. Meder and J. E. Purcell, Phys. Rev. C 12, 2056 (1975).

[12]F. D. Becchetti and G. W. Greenlees, Phys. Rev. 182, 1190 (1969).

[13]F. Ajzenberg-Selove, Nucl. Phys. A360, 1 (1981), P. M. Endt and C. Van der Leun, *ibid.* A310, 1 (1978).

[14]P. D. Kunz, computer code CHORK, modified by L. D. Rickertsen (unpublished).

[15]M. E. Rose, *Elementary Theory of Angular Momentum* (Wiley, New York, 1957).

[16]P. J. Ellis, Nucl. Phys. A302, 257 (1978).

[17]A. Bohr, Nucl. Phys. 10, 486 (1959).

[18]H. Nishioka, R. C. Johnson, J. A. Tostevin, and K.-I. Kubo, Phys. Rev. Lett. 48, 1795 (1982).

[19]B. Imanishi and W. von Oertzen, private communication.

[20]P. J. Brussaard and H. A. Tolhoek, Physica 23, 955 (1957).

[21]A. R. Edmonds, *Angular Momentum in Quantum Mechanics* (Princeton University Press, Princeton, New Jersey, 1957), Appendix 2.

[22]K. Alder, A. Bohr, T. Huus, B. Mottelson, and A. Winther, Rev. Mod. Phys. 28, 432 (1956).

[23]G. P. Ponzano and T. Regge, in *Spectroscopic and Group Theoretical Methods in Physics,* edited by F. Bloch *et al.* (Wiley, New York, 1968), p. 1.

[24]W. Bohne, K. Grabisch, J. Hergesell, Q. Liu, H. Morgenstern, W. von Oertzen, W. Galster, and W. Treu, Nucl. Phys. A332, 501 (1979).